26 April 1974, Volume 184, Number 4135 SCIENCE

The Oblateness of the Sun and Relativity

R. H. Dicke

Tests of general relativity fall into two classes: (i) the null tests, such as the Eötvös experiment, which test the broad principles of relativity, and (ii) the non-null tests, such as the gravitational deflection of light and the relativistic rotation of Mercury's perihelion, which generally test a specific theory, such as Einstein's gravitational theory. The gravitational red shift is an exception for it is a non-null test, but primarily of general principles.

The only existing accurate test (with a precision of ~ 1 percent) specific to Einstein's theory of gravitation is that based on the motion of Mercury's perihelion. However, in 1967 doubts about the validity of this test were raised by the publication (*1*) of the results of a measurement of the solar oblateness. The publication of this note led to a flood of correspondence and to the publication of at least 16 major papers by others attempting to find alternative explanations for the oblateness or otherwise raising questions about these observations. It is amusing to note that the publication (*2*) of our version of the Eötvös experiment, an experiment which supported Einstein's equivalence principle with an accuracy of one part in 10^{11}, did not cause the slightest ripple.

Responding to the published papers (*3*) greatly delayed the publication of a detailed analysis of the 1966 results, but the overall effect of these papers has been good. In analyzing the data we have benefited from consideration of the questions raised in these papers and this has affected our review articles (*4, 5*) and the comprehensive paper on the observations (*6*). It seems appropriate at this juncture to present an overview of our observations.

The author is Cyrus Fogg Brackett Professor of Physics at Princeton University, Princeton, New Jersey 08540.

We find that the implication of the solar oblateness for Einstein's theory seems even more serious now than it did 7 years ago. The observations have been studied exhaustively and a large number of possible complications in the interpretation of the data have been examined and eliminated. None of the alternative explanations of the oblateness signal has survived quantitative tests of its validity.

The general conclusion reached is that the sun had an oblateness of $\Delta r/r = 4.51 \pm 0.34 \times 10^{-5}$ in 1966 (*6*). (Here, $\Delta r = r_e - r_p$, where r_e is the equatorial radius and r_p the polar radius of the sun.) This represents an excess of 3.7×10^{-5} over the oblateness due to surface rotation. We have not yet been able to find any explanation for this excess oblateness except the existence of a solar quadrupole moment of $J = 2.47 \pm 0.23 \times 10^{-5}$.

If this explanation is correct, the implied rotation of Mercury's perihelion, 3 arc seconds per century, leads to a discrepancy of 7 percent in the relativistic part of the rotation of Mercury's perihelion. This discrepancy seems to be large enough to be of concern, but it is obvious that one should not discard general relativity or adopt a modified form of the theory without the support of other observations. Complementary observations of sufficient precision are not yet available. It will be interesting to see if the observations, when available, support these conclusions.

Under the scalar-tensor theory a 7 percent deficiency in the relativistic part of the perihelion rotation implies a 5.2 percent deficiency in the gravitational deflection of light (or microwaves) and the retardation of microwaves passing the sun. It seems likely that a definitive complementary observation will first come from this quarter.

Other oblateness observations are needed. Also, radar observations to an artificial planet in an inclined elliptical orbit would be very important. Such observations could provide highly precise measures of the motions of the perihelion and the node, permitting a separation of the relativistic and quadrupole effects.

While the validity of general relativity is the most important issue affected by our observations, many interesting problems concerning the physics of the solar interior are involved. Also, the significance of the observations can only be understood against a background of solar physics, and I briefly discuss these physical matters before turning to the observations.

History

A major scientific crisis developed in the middle of the 19th century when Leverrier (*7*) found that the planet Mercury apparently was not moving in accordance with the laws of Newtonian mechanics and Newtonian gravitation. The observed perihelion motion was in excess of that calculated from planetary motions. The excess motion of the perihelion that he found might have been explained if some extra perturbing mass in the solar system could have been located. A hypothetical massive planet *Vulcan* near the sun was never found, and a planetoid ring, sufficiently massive to induce the perihelion shift, would have scattered more light than a single planet and should have been visible. The great interest in this paradoxical result vanished in 1915 when Einstein showed that the excess motion of Mercury's perihelion could be explained as a relativistic effect (43.0 arc sec per century).

In recent years there has been a renewed interest in the "excess" perihelion rotation. This interest has resulted from the appearance of the scalar-tensor theories of gravitation (*8, 9*). These theories are relativistic and represent modifications of Einstein's general relativity in which the gravitational effects from a scalar field supplement those of Einstein's metric tensor. In one form of the scalar-tensor theory the scalar plays the role of potential, as in Newton's theory but treated relativistically. A fraction s of a body's weight is due to a scalar force acting on the body, where $s = 1/(2\omega + 4)$ and ω is the dimensionless coupling constant of the theory. This constant ω is unknown, but the range $5 \leqq \omega \leqq 9$ has been considered reasonable on various grounds (*9, 10*).

Under the scalar-tensor theory the paradox of the excess perihelion motion reappears, but in a mild form. The relativistic effect is now $43(1 - 4s/3)$ arc sec per century. For $\omega = 5$ it is 9.5 percent less than Einstein's value. Thus, 4 arc sec per century of the perihelion motion would remain unaccounted for.

With our present knowledge of the solar system it seems quite certain that an undiscovered mass sufficiently large to generate an additional 4 arc sec per century in the motion of Mercury's perihelion must be found inside the sun if it is to be found at all; that is, the sun must be distorted. The most likely distortion of the solar interior is a shortening along the rotation axis, giving a solar quadrupole moment.

The significance of an oblate sun vis-à-vis the Mercury perihelion problem was first recognized by the great 19th-century astronomer Simon Newcomb (*11*). It was not only the absence of the extra planet or the planetoid ring that led Newcomb to this idea. He realized that a planet or a planetoid ring in the ecliptic plane would induce a regression of the node of Mercury's orbit equal to the advance of the perihelion. Such a nodal regression was incompatible with the observations.

The equator of the sun is tipped 7¼° relative to the ecliptic, and the regression of the node on the solar equator due to a solar quadrupole moment becomes transformed principally into a decrease of the inclination of Mercury's orbit. If the quadrupole distortion of the sun is sufficient to advance the perihelion by 4 arc sec per century, the accompanying rate of change of the inclination of Mercury's orbit is -0.25 arc sec per century (*12*). Clemence (*13*) obtained -0.12 ± 0.16 arc sec per century from the observations.

Physical Problems

Many interesting physical questions are raised by the possible existence of a solar quadrupole moment. One's first instinctive reaction is to question the observability of the mass distribution deeply buried in the sun. However, we are not required to know the details of the mass distribution but only the quadrupole moment. The gravitational potential outside the sun is

$$\phi = -\frac{GM_\odot}{r}\,(1 - Jr_\odot{}^2\,P_2/r^2) \qquad (1)$$

where J is the quadrupole moment, G the gravitational constant, $M_\odot$ the sun's mass, $r_\odot$ the sun's radius, and r the distance from the sun's center; $P_2 = (3\cos^2\theta - 1)/2$ is the second Legendre polynomial, where θ is the polar angle in spherical coordinates.

It can be shown that J can be determined unambiguously from surface observations, at least in principle. We first consider the simplified situation when only pressure and gravitational stresses are present in the observed surface layers o^c^ the sun. The momentum balance conditions for a steady state are then (in these layers)

$$\nabla p + \rho\nabla\phi = 0 \qquad (2)$$

where p is the pressure and ρ the density of the solar atmosphere and ϕ *is* the gravitational potential. The gradients ∇p and $\nabla\phi$ are vectors normal to surfaces of constant p and ϕ, respectively. From Eq. 2 these vectors are parallel to each other and the two surfaces must coincide.

Forming the curl of Eq. 2 gives

$$\nabla\rho \times \nabla\phi = 0 \qquad (3)$$

implying that the vectors $\nabla\rho$ and $\nabla\phi$ are parallel and that the surfaces of constant ϕ are also surfaces of constant ρ. The gas in the outer 15 percent of the sun is believed to be in convective equilibrium, implying a thorough mixing and a uniform composition. Thus, the temperature $T = T(p, \rho)$ and p, ρ, and T are all constant on a surface of constant ϕ. This implies that these four quantities are functionally related and that

$$\begin{aligned} p &= p(\phi) \\ \rho &= \rho(\phi) \\ T &= T(\phi) \end{aligned} \qquad (4)$$

It has been shown (*14*) that for all reasonable values of J the limb of the sun is determined to a good approximation by a surface of constant density. Thus, the observed shape of the sun determines the shape of a surface of constant ϕ. Matching the oblateness of this surface of constant ϕ to the oblateness calculated from Eq. 1 yields the value of J.

The oblateness of the surface of constant gravitational potential is $\Delta r/r = (r_e - r_p)/r = \frac{3}{2}J$. To rotate the perihelion by 4 arc sec per century requires an oblateness of approximately 5×10^{-5} (*12*).

The discussion above is predicated on the assumption that only pressure and gravitational stresses occur in surface layers. But both velocity and magnetic fields are known to be present in a quasi steady state, and modern instruments provide detailed maps of their distributions in the photosphere.

When steady-state magnetic or velocity fields, or both, are present in a surface patch, Eq. 2 is modified by adding $\mathbf{F}$ to the left side, where $\mathbf{F}$ is the divergence of the stress density of these fields. The resulting modifications of p and ρ on surfaces of constant ϕ are (*5*)

$$\delta p = W \qquad (5)$$

$$\delta\rho = -\frac{1}{g}\,(F_3 + \partial W/\partial x^3) \qquad (6)$$

where g is the gravitational acceleration and $-F_i$ is the (covariant) force density due the magnetic or velocity fields. The generalized coordinates x^1, x^2, and x^3 are so chosen that x^3 is constant on surfaces of constant ϕ. From Eq. 2, F_α is derivable from a potential W on such a surface and $F_\alpha = -\partial W/\partial x^\alpha$, $\alpha = 1, 2$. Outside the surface patch W is defined to be zero.

From the equation of state, the changes in pressure and density inside the surface patch imply a change in temperature

$$\delta T = (T/p)\delta p + (T/\rho)\delta\rho \qquad (7)$$

on surfaces of constant potential. Thus, the brightness of the surface patch is generally affected by the surface field unless the field distribution is adjusted to keep T constant on surfaces of constant optical depth. A sunspot provides a striking example of the effect on brightness of a strong magnetic field in the surface layers.

It should be noted that the corrections to p and ρ occur in the surface layers only where the fields exist. Thus, a strong magnetic field in a sunspot cannot affect the brightness or the shape of the sun outside the sunspot, nor can a strong velocity field below the observed photospheric surface affect the shape, except through its affect on the mass distribution and hence its effect on the shapes of surfaces of constant ϕ.

Inasmuch as only the observable fields (in "seen layers") can disturb the relations given by Eq. 4, and the corrections to these relations can be explicitly calculated from the observable fields, the field-induced corrections to the oblateness are observable, in principle at least.

For the restricted problem of an oblateness induced by surface fields, the general theory has been developed (*14*). The conclusion reached from an analysis of the observations of the magnetic and velocity fields is that the only important surface field is the velocity field of surface rotation. This correction to the solar oblateness increases the oblateness by 0.8×10^{-5} (*14*). With this correction the oblateness is

$$\frac{\Delta r}{r} = \tfrac{3}{2}J + 0.8 \times 10^{-5} \qquad (8)$$

How is a solar quadrupole moment to be obtained? Strong internal stresses are required, for in their absence the sun rounds up to give a sphere as the shape of minimum energy. Both magnetic and velocity fields are possible sources of internal stress. A rapid rotation of the deep interior, the inner half (by radius) rotating 20 times as fast as the surface (1.35 days per revolution of the core), would generate a solar quadrupole moment large enough to give an oblateness of 5×10^{-5} from Eq. 8 (*15*).

For a magnetic stress the strength required depends on the magnetic configuration, but field strengths of the order of 10^7 gauss are required. These magnetic field strengths are so much stronger than any field observed in a low-density star that magnetic stress as a source of a solar quadrupole moment does not seem to be promising.

The first obvious question to be raised in connection with a rapidly rotating core in the sun is: How can the surface rotate so slowly if the interior rotates so rapidly? My colleague P. J. E. Peebles and I pondered this question in 1963 before there were any reliable measurements of magnetic fields in the solar corona. Despite the absence of observations, we concluded that the only reasonable source of a torque acting on the sun was the solar wind coupled to the sun by means of a twisted magnetic field. The magnetic field strength was estimated from the requirement that the magnetic pressure not exceed the gas pressure outside a magnetic strand (*12*).

Using the theory developed for the purpose and the estimated magnetic field strength, we obtained 5×10^{29} dyne centimeters per steradian for the torque density on the solar equator (*12*). It is remarkable that many years later, after the magnetic field observations were available and a more completely developed theory had been published (*16*), the torque density obtained from the observations was essentially the same, 6×10^{29} dyne cm ster^{-1} (*17*) [also see (*16*)].

A second remarkable coincidence in the 1964 paper (*12*) is the fact that the observations 2 years later (*1*) gave an oblateness only 20 percent less than the estimate used for modeling in the 1964 paper.

A third coincidence involves the solar interior and the 1964 torque estimate. It was found that the viscous drag of a rapidly rotating solar core on the slowly rotating outer solar shell represented a torque density of 3.5×10^{29} dyne cm ster^{-1} (*12*), essentially the same as the solar wind torque. With a more recent solar model this is 4.2×10^{29} dyne cm ster^{-1} (*17*). In obtaining these results it was assumed that the sun arrived on the main sequence with a steep angular velocity gradient at the surface of a rapidly rotating core and that this configuration was quasi-stable. The leakage of angular momentum from the core could be calculated because a totally ionized medium like the solar interior has a calculable viscosity.

The outer half of the sun (by radius) has a low average density and a moment of inertia so small that the solar wind torque would have slowed the rotation of this shell rapidly (*17*). One would expect a substantial part of the present loss of angular momentum to the solar wind to have its origin in viscous leakage from the core if the overall picture is correct.

To have enough angular momentum in a rapidly rotating core to generate an oblateness of $(4 \text{ to } 5) \times 10^{-5}$ requires a fairly steep angular velocity gradient. This raises questions of hydrodynamic stability that have not yet been completely resolved. It was early recognized that a rapidly rotating core must have its surface substantially below the outer convective layer of the sun to avoid the generation of turbulence by shear instability (*12*). The buoyancy force associated with vertical motion in a density-stratified fluid, such as the deep solar interior, strongly damps out the incipient motions of this type of instability.

It was not recognized at first that there was another type of instability, thermally driven, that under certain conditions would generate a slow turbulence in the fluid if the angular momentum (per unit mass) were to increase inwardly [Goldreich and Schubert (*3*)]. This instability is very weak and is easily terminated by a suitable motion of the fluid or a small vertical gradient in the mean molecular weight of the fluid. All that is required to protect the surface of a rapidly rotating core from this instability is a jump by $\sim 10^{-3}$ in the mean molecular weight across the boundary of the core. This slight change in molecular weight might have been obtained by mixing of the products of nuclear burning in the core of the young sun. It seems unlikely that our knowledge of the sun's history is sufficiently firm to exclude this possibility at this time.

Closely related to this instability are the Eddington-Sweet thermally driven circulation currents. These currents are usually considered to be too slow to be important, but it has been shown that they can become quite rapid when there is a steep angular velocity gradient (*15, 18*). These circulation currents can also be stopped by small molecular weight gradients (*15, 18*).

"Spin-down" currents were early suggested as a possible means of slowing the rotation of the solar interior [Howard *et al.* (*3*)]. These currents provide the means for the rapid slowing of rotation in a stirred cup of tea. It has been shown that in the density-stratified solar interior spin-down currents are greatly modified, being restricted to a very thin spherical layer at a spherical boundary (*19*). These currents are not believed to be significant for the solar model under consideration, remembering the great weakness observed for the solar wind torque.

When dealing with the solar interior one observation is worth a thousand calculations. Fortunately there are observations (other than the solar oblateness) which seem to have a bearing on the question of the rotation of the solar interior. Observations of other stars, particularly solar-type stars, provide several useful pieces of information. Rotation rates of stars substantially more massive than the sun are great

(Fig. 1). For stars slightly more massive than the sun ($\sim 1.2\,M_\odot$), Kraft (*20*) has found that the rotations are first rapid but then decrease as the stars age. Very young stars rotate about 20 times as fast as the present surface rotation of the sun. The rotation drops to one-half this value when the star is nearly 10^9 years old. For still older stars the rotation rate is even less (see Fig. 1).

From these and other observations a reasonable physical picture has gradually developed (*20*). For solar-type stars a convective shell is believed to exist at the surface. The turbulence of this convective layer sends shock waves into the upper stellar atmosphere. These shock waves heat the atmosphere to form a corona, driving a stellar wind and pulling out magnetic field strands into the stellar wind. The slowing of the surface rotation with time is believed to be due to the twisting of this magnetic field and the resulting stellar wind torque. If this picture is correct, we are now observing in stars the slowing of rotation believed to have occurred in the sun billions of years ago. The key question involves the interiors of these stars. Is a rapidly rotating core left in the interiors as the rotations of the surfaces of these stars decrease?

The answer to this question may be provided by the lithium abundance observed in these stars. In addition to the decrease in surface angular velocity, there is a decrease in the abundance of lithium at the surfaces of solar-type stars with age (*21*). This gradual disappearance of lithium seems to be associated with the loss of angular momentum, for it occurs only in stars that lose surface rotation [see (*20*) for references].

It has been shown that the loss of lithium can be quantitatively related to the loss of the surface angular velocity of these stars if the rotation of only an outer shell is decreased and the angular momentum is transferred from the interior of the star by an isotropic turbulent diffusion process (*17*). The fluid motion that carries angular momentum to the star's surface also carries lithium to the inner half of the star (by radius) where it is rapidly burned.

In the sun lithium has been depleted by a factor of ~ 200, suggesting that the same process has occurred there. The same turbulent diffusion model gives a quantitatively satisfactory relation between the solar wind torque and the rate of loss of lithium at the sun's surface (*17*). If this turbulent diffusion takes place, it is very likely generated by the Goldreich-Schubert mechanism (*3*).

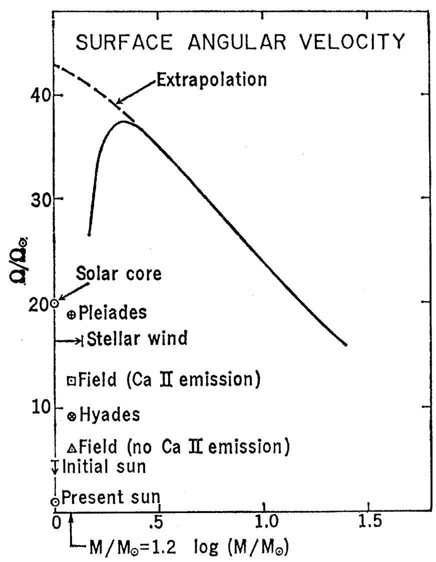

Fig. 1. Stellar angular velocities; Ω and M are the surface angular velocity and mass of the star, and $\Omega_\odot$ and $M_\odot$ are the surface angular velocity and mass of the sun. The Pleiades are young and the Hyades are $\sim 9 \times 10^8$ years old. Field stars with Ca II emission lines are younger than those without.

Fluid motion is not the only possible means of transport of angular momentum in the sun. It could be transported by twisting internal magnetic fields, or by means of internal hydrodynamic waves, but then we would have neither a means for depleting lithium nor an explanation for the relation between the depletion of lithium and the transport of angular momentum.

The observations of the loss of surface rotation of solar-type stars, the depletion of lithium in these stars, the solar wind torque and the resulting loss of angular momentum from the sun, and the depletion of lithium from the sun, together with the solar oblateness observations to be discussed below, permit the construction of a crude model for the internal rotation of the sun. To be believable, such a solar model must be the end result of a possible solar history.

The first attempt at constructing such a history and a rotation model was made before either the solar wind torque or the oblateness were known (*12*). The slowing of the rotation of solar-type stars on the main sequence was also unknown, and the significance of the depletion of lithium in this connection was not appreciated. Making the hypothesis that the solar oblateness, if found, would be $\Delta r/r = 6 \times 10^{-5}$ led to a rotational model based on rather crude numerical estimates. In this model the core had a radius of $\sim 0.75\ r_\odot$ and an angular velocity 25 times as great as that of the surface (*12*). The observations since 1964 have changed the model, but not dramatically. It is now suggested that the core radius is $\sim 0.5\ r_\odot$ and that the angular velocity is 20 times the surface value (*17*).

In constructing a possible solar rotational history all of our present knowledge is used, but it must be emphasized that any such history can be at best fragmentary and tentative. We observe only a very thin layer at the sun's surface. From this we are trying to picture not only the nature of the rotation of the solar interior but the past history of this rotation. It is obvious that this is risky.

The sun is believed to have started its life as a greatly expanded, completely convective red star (Fig. 2). To be hydrodynamically stable it would have been substantially uniform in its rotation.

The contraction of the deep solar interior is believed to have "spun-up" the solar core and decreased the logarithmic temperature gradient, eliminating convection as the means of energy transfer from the deep solar interior. The density stratification of this state stabilized the deep interior against the more violent of the hydrodynamic instabilities, permitting large angular velocity gradients to exist, at least for times of the order of the thermal relaxation time ~ 30 million years. Relaxation times of 10^{10} years require stabilization against the thermally driven instabilities. Such stabilization could have occurred in several different ways, including the development of a jump in mean molecular weight $\Delta\mu \sim 10^{-3}$ across the core boundary (see Fig. 3).

If the thermally driven instabilities were to have been eliminated, leading to an angular velocity distribution roughly like curve (c) of Fig. 3, the angular momentum lost from the core by diffusion would probably have been transported to the convective zone by the Goldreich-Schubert turbulence phenomenon, leading to the gradual depletion of lithium. As angular momentum was lost by diffusion from the surface of the rapidly rotating core, the angular velocity gradient at the core's surface decreased and the rate of loss of angular momentum decreased.

Numerous numerical variations of this history have been examined (*17*). The initial solar surface rotation was varied and the solar wind torque was assumed to be proportional to either the angular velocity of the surface or the square of the angular velocity. The initial surface rotations range from two to ten times the present rotation. The model parameters were adjusted to yield the observed present rotation and the observed surface value of the lithium abundance. Without any more adjustment of parameters, the present value of the solar wind torque density was calculated. This calculated torque density ranges from 4.5×10^{29} to 9.0×10^{29} dyne cm ster^{-1} (*17*) (to be compared with the "observed" value of 6×10^{29}). It is an amusing thought that, if this model is correct, the solar wind torque can be calculated from the rotation rate of the sun and the abundance of lithium at the sun's surface.

It is within the context of the above physical picture that the solar oblateness observations should be examined. The suggestion that the sun's internal rotation (and quadrupole moment) is great enough to account for all the excess motion of Mercury's perihelion (*22*) does not seem to be compatible with the observational limits on the rate of change of the inclination of the orbit (*12*), but there seems to be no insurmountable physical difficulty associated with the assumption that the sun has an oblateness of $\sim 5.8 \times 10^{-5}$, sufficient to rotate Mercury's perihelion by ~ 4 arc sec per century. [See (*23*) for other discussions of physical problems associated with rapid internal rotation.] See (*15*) for review articles.

Observational Problem

The measurement of the solar oblateness with an accuracy of $\pm 0.5 \times 10^{-5}$ imposes a severe observational requirement. This precision represents an accuracy of ± 0.005 arc sec in the difference in equatorial and polar radii. (An oblateness of 5×10^{-5} implies a radial difference $\Delta r = r_e - r_p = 0.048$ arc sec for $r = 960$ arc sec.)

In order to avoid an enormous distortion of the sun's image by atmospheric refraction, the sun should be high in the sky, with a zenith angle less than 60°. But this implies a turbulent atmosphere heated by the sun and

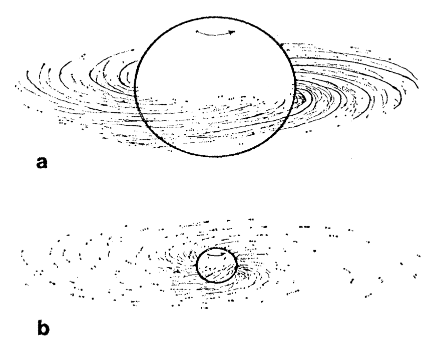

Fig. 2. (a) A schematic view of the sun during its expanded Hayashi phase showing the hypothetical twisted magnetic field pulled out by the solar wind. (b) The same after some contraction of the sun has occurred.

a substantial distortion of the "seeing" at the solar limb. A continually fluctuating solar limb fuzzed out by several seconds of arc is the normal appearance of the sun under these conditions. We are demanding a measurement of limb position to an accuracy of 0.1 percent of the width of this continually varying, ill-defined edge of the sun.

Obviously a single measurement is not capable of this precision, but the mean value of a long series of observations carefully controlled to avoid instrumental, atmospheric, and personal bias might yield the necessary accuracy. To avoid personal bias the instrument

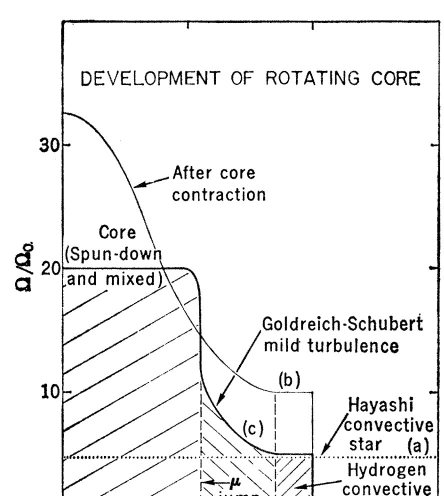

Fig. 3. Hypothetical history of the sun's rotation. The angular velocity Ω as a fraction of the present surface angular velocity Ω_0, is plotted as a function of radius (with $r = 1$ at the surface). The three curves show the distributions of angular velocity: (a) during the pre–main sequence Hayashi phase, (b) after arriving on the main sequence, and (c) after several thermal relaxation times.

should obtain the data as much as possible "untouched by human hands." There are statistical reasons to believe that the old 19th-century observations of the solar oblateness with a "heliometer" may have suffered from personal bias (*24*).

These considerations impose severe requirements on the measuring instrument. The following is an incomplete list:

1) The difference between the equatorial and polar radii must be determined to a precision better than a wavelength of light for the solar image 6.8 cm in diameter actually used.

2) The sensitivity of the measuring instrument must not drift more than a few parts per million between the determination of the measures of r_e and r_p.

3) The astigmatism of optical components must be eliminated as a factor affecting the apparent oblateness. The astigmatism of a flat mirror ~ 50 cm from the telescope objective should be eliminated (or determined) to a radius of curvature of 100 km (representing a 10^{-2} wavelength dip in the surface of an 8-cm mirror).

4) For the integration techniques used, the transmission by the optical system of the light rays from the limb near the pole and near the equator should not differ by more than 0.03 percent.

During the early phases of this experiment, when the oblateness telescope was being designed, constructed, and tested, H. M. Goldenberg and I had the invaluable help of H. Hill, now at the University of Arizona. Many of the clever innovations in the instrument are due to him. The high quality of the data is also due in part to the skill of our graduate student assistants, P. Boynton, K. Davis, B. Godfrey, P. Henry, E. Holm, E. McDonald, and R. Stokes.

It seemed best to us to use a technique based on integration rather than differentiation to determine the position of the solar limb. The sun's image is projected onto an occulting disk slightly smaller than the sun's disk and accurately centered by a servomechanism (see Fig. 4). The light from the 6 to 19 arc sec of the sun's disk that projects beyond the occulting disk is used as a measure of the amount of projection of the limb. The distribution of the light flux per unit angle about the solar limb is obtained photoelectrically, by using a rapidly rotating scanning wheel perforated by two diametrically opposed apertures. For an oblate sun slightly more light would be transmitted to the photocell when the apertures in the wheel sample light obtained from the equatorial regions. (The same would be true if the solar equator were brighter than the pole. I shall return to a discussion of this ambiguity.)

Integration is very much superior to differentiation. The poor seeing which fragments a point of light from the solar limb into a disorganized patch of light several seconds of arc across does not change the integral (namely, the light flux), whereas the differential of surface brightness is very sensitive to this fragmentation. The integral is affected by this fragmentation only to the extent that the gradient of the brightness of the sun's disk varies with radius at the edge of the occulting disk.

To some extent the fragmentation of the image from a point source of light is systematically elongated in one direction by anisotropy in the atmospheric turbulence at the observatory. This elongation can affect the apparent oblateness (again only when the gradient in solar brightness varies radially at the edge of the occulting disk). I shall return to this problem.

Fragmentation of the image is not the only atmospheric problem. A temperature difference between the inside and outside of the observatory causes the air at the entrance to act like a very weak cylindrical lens that distorts the solar image. I shall return to this difficulty.

A second advantage of the scanning technique is the rapid intercomparison of the light flux from the equator and the pole, effectively measuring the radial difference ($\Delta r = r_e - r_p$) 244 times per second.

Two numbers are required to define the oblateness. These numbers can be taken to be the magnitude of the oblateness and the orientation of the minor oblateness axis. An alternative and more useful way of expressing the oblateness is in terms of two orthogonal components. For reasons to be discussed below, the measured oblateness is expressed in terms of the following two orthogonal components: a shortening along the north-south diameter of the solar disk and a shortening along the northeast-southwest diameter. The former radial difference defines the "vertical component" of the oblateness ($\Delta r_v = r_{E\text{-}W} - r_{N\text{-}S}$) and the latter is

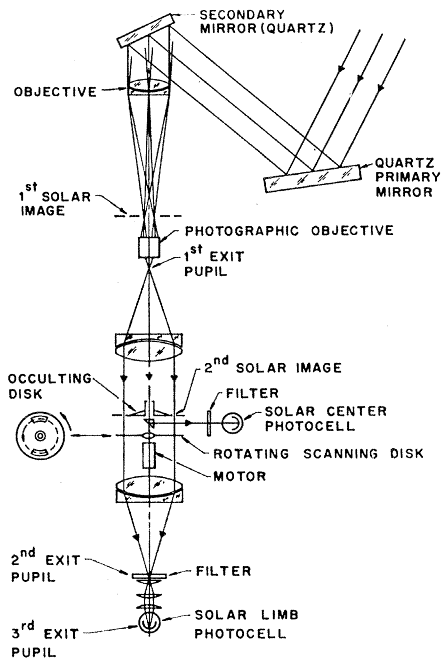

Fig. 4. Optical system of the solar oblateness telescope.

called the "diagonal component" of the oblateness ($\Delta r_d = r_{NW\text{-}SE} - r_{NE\text{-}SW}$).

The vertical and diagonal components of the oblateness are not determined from point to point measurements made at the ends of the diameters, but from the sine and cosine components of the 244-hertz signal in the photocurrent. A two-phase lock-in amplifier is used to continuously measure these sine and cosine components.

The requirement for great precision in the occulting disk, for lenses free of astigmatism and uniform in optical transmissions, and for numerous other tight mechanical tolerances can be obviated by the simple expedient of using the instrument in such a way that errors from these components average to zero. The telescope and all its associated equipment is made to rotate rigidly about the optic axis of the system. All errors associated with the telescope and its equipment disappear from data combining results obtained with the telescope in positions 90° apart. A concern that the gravitational distortion of the optical and mechanical systems might change under this 90° rotation is eliminated by mounting the telescope with its optic axis vertical and using two mirrors to direct the sun's light into the telescope.

Unfortunately, the error due to astigmatism in these plane mirrors is not eliminated by this rotation procedure. But the astigmatic error is eliminated by rotating the two mirrors about normals to their surfaces, observations being made equally frequently with these mirrors in each of two positions 90° apart. The primary (p) mirror is rotated every two observational days at the start of the day. The secondary (s) mirror is rotated every observational day at noon. Correlations of mirror functions describing the mirror orientations ($f_p = \pm 1$, $f_s = \pm 1$) with the data residuals permit a determination of these astigmatic corrections, which can then be subtracted from the data (if desired). In any case, these errors average to zero over the whole observational season (3½ months in the summer of 1966).

One mirror error is not eliminated by this procedure. A slight, axially symmetric concave or convex shape of the mirror surface induces an astigmatic distortion of the sun's image when the mirror is used off axis (that is, with nonnormal incidence). This distortion is unaffected by mirror rotation.

A convex primary mirror with a radius of curvature of 55 km would produce an off-axis distortion of the sun $(\Delta r/r)_v = 0.73 \times 10^{-5}$ on 1 July. On 1 October this becomes 1.52×10^{-5} [see (*6*)].

At this point I should mention one of the great advantages of our particular choice of the orientation of the axes of the oblateness components. The above distortion appears wholly in the vertical component of the oblateness and the diagonal component is free of the distortion. On symmetry grounds one would expect the true solar oblateness to have a minor axis along the rotation axis of the sun. In any case we make this assumption. Thus, only one oblateness component (diagonal or vertical) is needed to determine the solar oblateness. If the diagonal component is used, the oblateness determination is free of mirror distortion.

There is another important advantage in using this component. The important parts of the observatory and the optical system exhibit symmetry under reflection in a plane containing the optic axis and the north-south line. It was noted above that there are two types of distortion of the solar image induced by temperature inhomogeneity at the observatory. One of these is due to an anisotropic spreading of a point light source. The other is a "cylindrical lens effect" due to a temperature difference between the inside and outside of the observatory. Both of these effects exhibit the symmetry of the observatory, and at noon these effects disappear from the diagonal measure of the oblateness. These seeing contributions to the diagonal component are odd functions of the time of day relative to noon, and prior to 1 September (while the sun is high in the sky) they are observed to be relatively minor (*6*).

A third advantage in a determination of the solar oblateness based on the diagonal component is the fact that this component is expected to vary strongly through the season as the earth swings around the sun and we observe the tilted solar axis from various directions. The form of this expected variation is known and the amplitude can be determined independent of any constant bias introduced by the atmosphere or the instrument.

A fourth (relatively minor) advantage of using the diagonal component is that the effect of gross laminar refraction by the atmosphere on the shape of the sun is an odd function of time for this component, and a minor error made in determining its magnitude is of no great consequence. Such an error would average to zero.

I do not want to imply that the vertical component of the oblateness is useless. The mirror distortions have been determined and a procedure has been devised for extrapolating the daily observations to the beginning of the day to substantially reduce the effects of turbulence at the observatory (*6*). The oblateness measures based on both the diagonal and the vertical component are presented below.

I return now to the integration technique discussed above. The advantages of this technique are great but it carries one disadvantage. A 244-hertz signal can be obtained from either an oblateness or a brightening of the sun in the equatorial region. I shall call the latter a "brightness signal" and the former an "oblateness signal."

This ambiguity concerned us from the beginning and we designed the experiment in such a way as to do all we could to separate these two effects. The oblateness signal is proportional to both the oblateness and the brightness of the sun at the edge of the occulting disk, whereas the brightness signal increases with the amount of exposed solar photosphere, being proportional to the light flux for simple equatorial brightening independent of position relative to the limb.

In order to reduce the brightness signal to a minimum, observations were made with the limb as close to the edge of the occulting disk as possible without cutting into the seeing distribution at the limb. This distance averaged to 6.4 arc sec over a random set of 26 days during the 1966 season. But to obtain a measure of the amount of brightness signal, measurements were also made with more of the photosphere exposed. The observational time was divided equally among exposures of 19.0, 12.7, and 6.4 arc sec of the solar disk. These three exposures are averages and are designated magnifications 1, 2, and 3 of the solar disk, respectively. For these three exposures a simple equatorial brightening produces signal intensities in the approximate ratios 3 : 2 : 1, respectively.

As a second test for a brightness signal, the occulting disk is replaced by a solid disk with an aperture in the form of a thin annular gap (14 arc sec wide) placed completely on the solar disk, near the limb but with the solar limb completely covered (*6*). This configuration minimizes the oblateness contribution to the total signal inasmuch as the positive oblateness signal derived from the inner edge of the annulus is nearly canceled by the negative signal derived from the outer edge. With the masking oblateness signal minimized the brightness signal is exposed. Very little time was devoted each day to this observation, but the time was sufficient to complement and support the other determination of the brightness signal with the occulting disk.

Oblateness Data

The reflection symmetry of the observatory, which, as discussed above, eliminates several biases of the diagonal component of the oblateness at noon, makes it desirable to project each day's observations of the diagonal component to noon. This projection would not be necessary if the observational day had equal numbers of observations in the morning and afternoon, but frequently poor weather forced an unbalanced day for which the biases would not average to zero.

Each observation of the solar oblateness requires approximately 2 minutes, and combines the data from two integrations with telescope positions 90° apart. The observations carried out at each of the three magnifications are averaged in three sets of hourly bins. Each of these three sets of hourly averages is then fitted by least squares by the function $a_t + b_t t$, where t is the time in hours past noon. The projection of the data to noon is accomplished by adopting the three values of the constant a_t for each day as the measures of the diagonal component of the oblateness for that day at the three magnifications.

When the hourly averages of the diagonal component of Δr, $\Delta r_d = (r_e - r_p)_d$, are averaged over the observational season, the values obtained for a_t and b_t for the three magnifications are $a_t = 0.007 \pm 0.001$, 0.005 ± 0.001, and 0.005 ± 0.003 arc sec and $b_t = -0.003 \pm 0.0005$, -0.0006 ± 0.0006, and -0.0005 ± 0.001 arc sec per hour for magnifications 1, 2, and 3, respectively. [See (*6*) for the details.]

The daily values of a_t are plotted in Fig. 5 as a function of day number d, where $d = 1$ on 1 May 1966. The error flags are standard deviations derived from the least squares fits. Prior to $d = 43$ substantial modifications of the apparatus were being made to eliminate servo difficulties and other problems, and a regularized observational procedure had not been adopted. These days are dropped. Toward the end of the season the sun was quite low in the sky and there are several indications that the data for $d > 140$ are less reliable than the rest. Dropping these data reduces the value of the inferred oblateness, but only by 10 percent.

As noted above, the assumption that the minor oblateness axis coincides with the solar rotation axis yields the time dependences of the diagonal and vertical components of the oblateness. For example, on 7 July the rotation axis is in the north-south direction and the diagonal component of the oblateness should be zero. The theoretical curve shown in each part of Fig. 5 is derived from the known orientation of the polar axis, assuming that the equatorial radial excess $\Delta r = r_e - r_p = 43.5$ arc msec $= 0.0435$ arc sec. Here the ordinate of this curve is given by $\Delta r \cdot f_d$, where f_d is defined by

$$f_d = \frac{1}{2} \sin 2P(\cos 2B + 1) \qquad (9)$$

and P and B are the standard position angles of the sun's rotation axis defined in (*6*).

The function

$$\Delta r_d = \Delta r \cdot f_d + c \qquad (10)$$

Table 1. Oblateness and other constants from Eqs. 10, 11, and 12. In a_{t1}, a_{t2}, and a_{t3}, the numbers 1, 2, and 3 stand for magnification numbers. The data in the range $43 \leq d \leq 140$, including only days with at least two magnifications, are used. N.D., not determined.

Data	Δr (arc msec)	c (arc msec)	c_f	c_s
a_{t1}	50.2 ± 7.4	−1.2 ± 2.9		
a_{t2}	42.8 ± 6.7	−3.1 ± 2.7		
a_{t3}	39.4 ± 6.5	−2.0 ± 2.6	0.097 ± 0.024	
a_{t1}	40.6 ± 6.8	1.1 ± 2.6	.037 ± .025	
a_{t2}	39.3 ± 7.1	−2.3 ± 2.7		
a_{t3}	38.0 ± 6.9	−2.5 ± 2.7	.017 ± .026	
a_{t1}	40.7 ± 6.8	0.6 ± 2.6	.083 ± .028	0.032 ± 0.031
a_{t2}	39.3 ± 7.2	−2.1 ± 2.8	.040 ± .030	− .008 ± .030
a_{t3}	38.4 ± 6.9	−3.3 ± 2.7	.036 ± .033	− .001 ± .030
a_{t1}	39.5 ± 6.8	1.3 ± 2.6	.109 ± .024	
a_{t2}	38.9 ± 7.1	N.D.	N.D.	
a_{t3}	37.8 ± 6.9	N.D.	N.D.	

fitted by least squares to the data for $43 \leq d \leq 140$ gives the results tabulated in the first three lines of Table 1 [see (6)]; c is a coefficient.

By intercomparing the values of Δr from Table 1, it is seen that the difference between the values of Δr for magnifications 1 and 3 is only marginally significant (1 sigma). Thus, there is no clear indication in this difference of any equatorial brightening of the photosphere (that is, a brightness signal). In the next section a more sensitive test for a brightness signal is discussed.

The results of the annular ring measures of equatorial brightening are briefly discussed in the next section. Reference should be made to (6) for the details.

The daily values of the vertical component of the oblateness are plotted in Fig. 6 for all three magnifications together with a curve for the vertical component based on $\Delta r = 0.050$ arc sec (6). The details of the extrapolation and fitting procedures are discussed in (6). The plotted points contain (small) corrections for the effect of faculae.

Effect of Atmospheric and Solar Disturbances

The possibility that atmospheric or solar phenomena might bias the oblateness data was of considerable concern to us from the beginning. While the oblateness data were being obtained, records of wind velocity, temperature, humidity, pressure, and atmospheric transparency were also obtained, the latter four parameters being measured at the observatory.

Owing to the sensitivity of the servo system to disturbances by wind, an attempt was made early to detect a wind-induced bias of the data. Such a bias was not found. In similar fashion a correlation of the oblateness with observatory temperature was sought. Again a null result. Later, a more severe test was provided by the correlation with atmospheric transmission.

It has long been known that a slight atmospheric haze steadies the solar image, and this was certainly our experience. Usually the notation in our log book that the sky was clear and blue with the air cool and dry was accompanied by the note that the seeing was poor.

I was surprised to discover that there is no hint of a correlation of the atmospheric transparency (haze index) with the oblateness (6). Before this statistical study it had been assumed that the large fluctuation in the solar oblateness seen in Fig. 5 in the range $d \geq 43$ was mainly due to poor seeing, but it was then found that a substantial part of this fluctuation is solar in origin (25) and periodic. This periodic fluctuation has not yet been traced to any observed feature of the sun's surface. (See discussion below.) To summarize, none of the five atmospheric parameters examined have shown any significant correlation with the observed oblateness signal.

The role of sunspots and other blemishes on the sun's surface vis-à-vis the solar oblateness signal was an early concern of ours (and also of many others, if letters and questions from colloquium audiences are any indication). The possibility that the oblateness signal might be biased by sunspots, faculae, prominences, a latitude variation of chromospheric line strengths, other chromospheric irregularities, a slight variation of the photospheric brightness associated with large patches of weak magnetic field, and other solar phenomena was early considered and analyzed (4, 5). To assist with the analysis, functional indicators of sunspots, faculae, prominences, and weak magnetic fields were constructed from the daily solar maps of the Fraunhofer Institute, Freiburg, Germany, and from daily magnetic maps supplied by R. Howard of Mount Wilson Observatory, California. The oblateness data were tested for contributions from these factors by evaluating the correlation coefficients of the oblateness fluctuation with these functional indicators.

These correlation coefficients provide more sensitive tests for these specific sources of brightness signal than does the variation of the oblateness signal with the amount of exposed photosphere. For example, the arrival of a sunspot at the solar limb occurs at a specific time and its influence at that time could be great, whereas averaged over the season it might be unimportant.

The correlation analysis and other analyses carried out before 1970 indicated that none of these solar phenomena were important (4, 5). Only the sunspot and facular functions showed significant correlation coefficients, and the indicated effects on the solar oblateness were substantially less than 10 percent.

Chapman and Ingersoll (3) have independently constructed a facular function that appears to be better than ours. It is derived directly from the solar photographs rather than from maps and yields a stronger correlation. Using their function, I found that approximately 10 percent of the oblateness signal is due to faculae (26, 27).

The solar oblateness Δr derived from the diagonal oblateness component and corrected for the effect of faculae can be obtained by fitting (by least squares) the function

$$\Delta r \cdot f_d + c_f F_c + c = \Delta r_d \quad (11)$$

to the daily values of Δr_d for $43 \leq d \leq 140$, where F_c is the Chapman-Ingersoll facular function (6). The results are given in Table 1, rows 4 to 6.

The sunspot function S is included by fitting the function

$$\Delta r \cdot f_d + c_f F_c + c_s S + c = \Delta r_d \quad (12)$$

to the data. The results are given in rows 7 to 9 of Table 1. It should be noted that the effect of adding the sunspot function is minor and that the coefficient c_s is not statistically significant.

It has been suggested that, owing to error in the facular function F_c, the corrections to Δr listed in Table 1 are lower bounds and that these corrections could be very much larger (*28*). By combining analyses based on F_c with those based on our facular function it has been shown that the correction due to error in F_c is minor (*27*), 2 to 3 percent. The results including this correction are given in rows 10 to 12 of Table 1. The average of Δr in these rows is 12 percent less than that in the first three rows.

It should be noted from Table 1 that after the effect of solar faculae is subtracted the marginally significant variation of Δr with magnification number disappears. Thus, there is no indication of an additional source of brightness signal. This interpretation is supported by the data obtained with the annular aperture. It is found that after the facular-correlated signal is subtracted from these data only noise fluctuations remain (*6*).

The values of Δr given in the last three lines of Table 1 are plotted as the upper points in Fig. 7. The error flags are discussed below. Curve A represents the constant value expected if these plotted points represent an oblateness signal. Curve B represents the curve expected if these plotted points do not represent an oblateness but rather a residual facular signal. The lower points on which B is based are facular signals obtained from c_f (lines 4 to 6) of Table 1. These points are normalized to permit B to cross A at magnification 1. Curve C represents the effect of a brightness signal due to a temperature excess in the equatorial regions. Curve D represents a brightness signal due to an equatorial temperature excess confined to the top 1 percent of the photosphere [(*29*); also see Durney and Roxburgh, Ingersoll and Spiegel, Durney and Werner, and Durney in (*3*)]. Clearly the oblateness data fit curve A best and are incompatible with curve B.

It has been suggested (*28*) that the strong increase in the facular signal

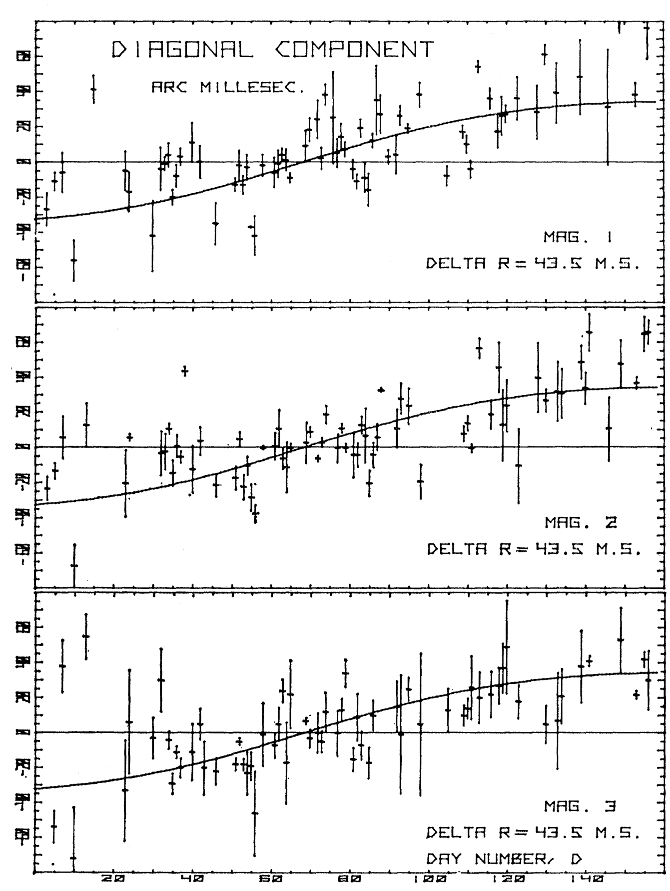

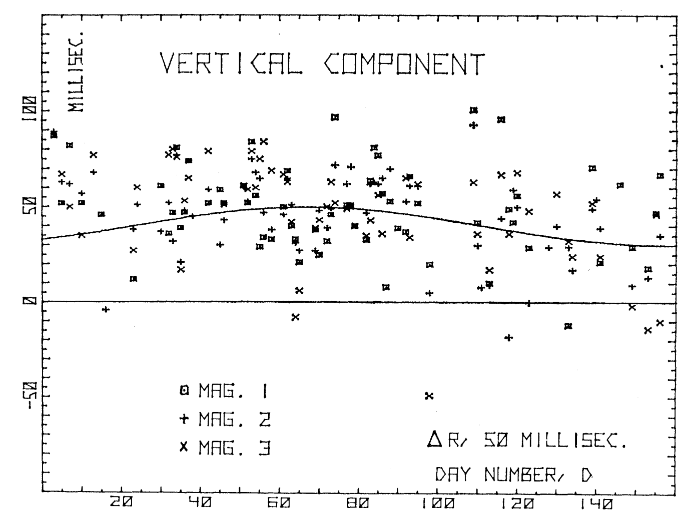

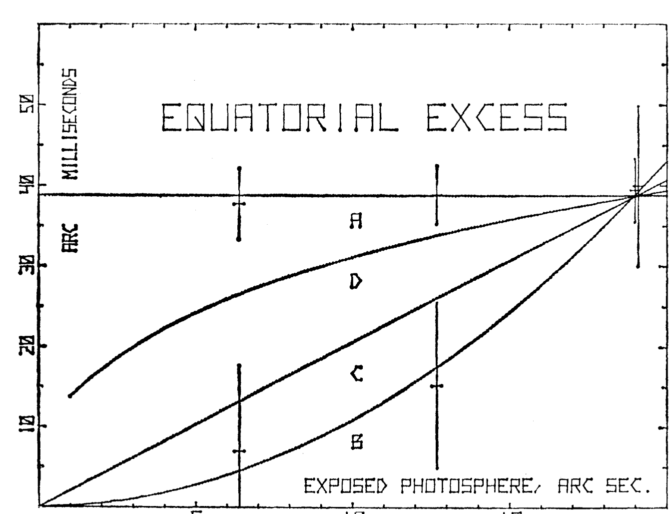

Fig. 5 (left). The diagonal component of the solar oblateness as a function of day number ($D = 1$ on 1 May 1966). Approximately 19.0, 12.7, and 6.4 arc sec of the photosphere are exposed beyond the occulting disk at magnifications 1, 2, and 3, respectively. For the theoretical curve an excess equatorial radius of $\Delta R = 43.5$ arc msec is assumed. Fig. 6 (top right). The vertical component of the oblateness as a function of day number. Results at all three magnification numbers are plotted. Fig. 7 (bottom right). The upper points (small error flags) represent the excess equatorial radius, Δr, in milliseconds of arc derived from least squares fits to the data of Fig. 5 after correction for facular signal. The points should fall on curve A if the residual is due to oblateness, B if it is due to uncorrected faculae, C if it is due to equatorial excess temperature, and D if it is due to excess temperature in the upper atmosphere ($\tau < 0.01$). Curve B is obtained from a quadratic fit to the three facular signal points c_f of lines 4 to 6 (Table 1) renormalized. These are the points with large error flags.

(measured by c_f, Table 1 and Fig. 7) with increasing exposure of the photosphere is due to an improved match of the strip of the photograph read to obtain F_c with the strip sampled by the rotating wheel of the telescope. However, it has been shown that the match is actually best for the least exposure (magnification 3) and is poorest for magnification 1 [see (*27*)]. The observed variation of the strength of the facular signal with the amount of exposed photosphere is consistent with what is known about the facular brightness near the limb (*30*).

I conclude from Fig. 7 that after the oblateness signal is corrected for contamination by the brightness signal from faculae the variation of the signal with limb exposure is consistent with the assumption that the residual signal represents pure oblateness. The assumption that the residual signal is due to faculae (curve B) seems to be contrary to the facts. The assumption that the residual signal is due to an equatorial excess temperature in the upper photosphere (curve D) is in fair accord with the plotted oblateness points, but the required variation of temperature with latitude is much greater than the variations observed even higher in the atmosphere (at optical depth $\tau \sim 0.001$) (*31*). Also, the energy required to maintain this temperature difference is excessive and there is no presently known stress to support the resulting pressure gradient [(*29*), but see Durney (*3*)].

As mentioned above, the large day-to-day fluctuation of the diagonal component of the oblateness has not been traced to either atmospheric fluctuation or observable solar features. In particular, only 17 percent of the mean square fluctuation seems to be due to the presence of faculae at the limb.

One striking feature of the remainder of the fluctuation (the contribution of faculae having been subtracted as discussed above) is the strong correlation between the fluctuations of the oblateness at different magnifications (*6*). Even more striking is the fact that much of this correlation is due to a strongly peaked function that is periodic with a 25⅔-day period (*6, 25*). It must be emphasized that the periodicity found is not simple; that is, it is not a simple sinusoidal oscillation with time. Instead, the periodic function is a highly irregular function which is repeated every 25⅔ days.

This periodic function is exhibited by "folding" the oblateness fluctuation at this period (that is, by averaging day-by-day the data that occur on each day with data 25⅔, 51⅓, . . . days earlier or later). Such a folded function is exhibited in Fig. 8. For fractional days the nearest integer is adopted as the (integral) day number d (*32*).

To exhibit the periodicity the "periodic autocorrelation" function is evaluated (*33*) (see Fig. 9). The probability of the occurrence of a 4-sigma peak at $P = 25⅔$ days with "data" drawn

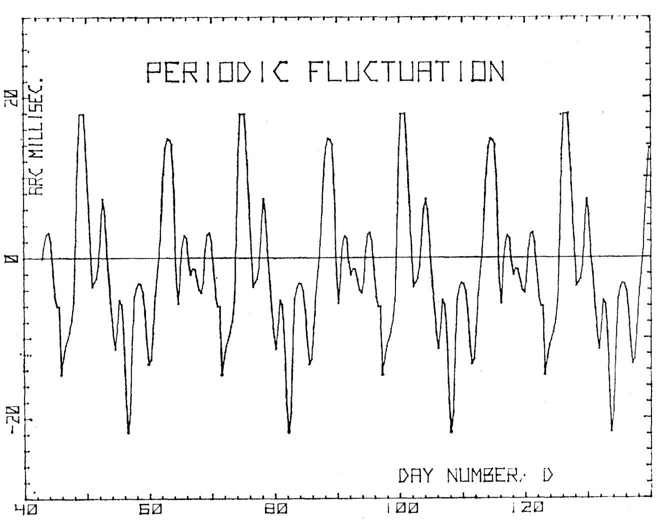

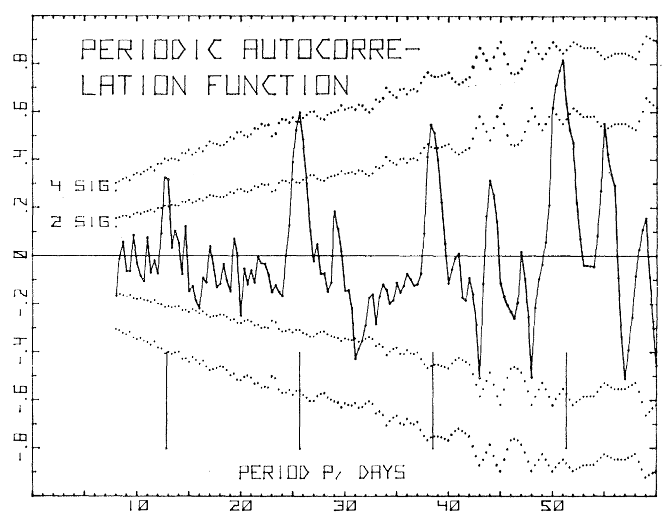

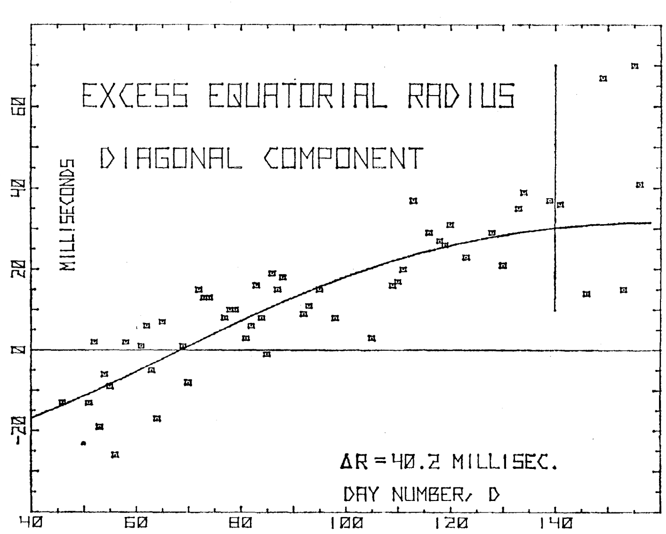

Fig. 8 (left). The periodic component of the fluctuation of the diagonal oblateness component at a period of 25⅔ days. Fig. 9 (top right). Periodic autocorrelation of the fluctuation in the diagonal component of the oblateness (after subtracting the contribution due to faculae). The 25⅔-day period is significant at the 4-sigma level. Fig. 10 (bottom right). The diagonal component of the oblateness (the average of the values at all three magnifications) with the facular signal and the periodic fluctuation subtracted. The defective data with $D < 43$ have been omitted; ΔR is the excess equatorial radius.

from a normal distribution is less than 3.6×10^{-4} and greater than 3×10^{-5} (*33*).

One surprising feature of Fig. 8 is the strong subperiodicity at 12⅚ days. Another surprising feature is the fact that a 25⅔-day period is shorter than the rotational period of the sun at any latitude, although the equatorial period is close (26.9 days). The subperiodicity seems to be due to the double-peaked structure of the periodic function (Fig. 8).

The periodicity seems to be due to shallow hills and valleys arriving at the solar limb at a latitude of roughly $\pm 45°$, where the rotational period is approximately 30 days. This periodic fluctuation is apparently missing from the vertical oblateness component.

It has been suggested that this periodicity is due to faculae (*28*), but the solar rotational period at the active solar latitudes is ~ 27.8 days instead of 25.7 days. Also the periodic correlation function computed from the fluctuation of F_c does not correlate significantly with the curve in Fig. 9. Furthermore, the folded function derived from the fluctuation of F_c does not correlate significantly with the folded function of Fig. 8 (*34*).

By correlating the periodic (that is, folded) function (Fig. 8) with the fluctuations in the diagonal oblateness component at each of the three magnifications it is shown that the periodic components at all three magnifications are equal to the statistical accuracy of the data. This indicates that the fluctutions are probably due to changes in shape, not to bright or dark spots appearing at the solar limb. Such spots would affect the data most strongly at magnification 1. (The facular signal at magnification 3 seems to be only 0 to 30 percent of that at magnification 1.)

The periodic fluctuation is strong, with a variance in the mean three times as great as the fluctuation due to faculae. If the periodic part of the fluctuation in the diagonal component of the solar oblateness is subtracted, the residual fluctuation seems to show no more interesting statistical properties and may be presumed to be random noise.

The average of the diagonal component of the oblateness over all three magnifications, with both the facular signal and the periodic fluctuation subtracted, is plotted in Fig. 10. The fluctuation of these data is much less than that seen in Fig. 5. The standard deviations shown as error flags in Fig. 7 represent errors after the correlated fluctuations are removed (*6*).

The value of the equatorial excess Δr determined by least squares by fitting Eq. 10 to these data for the range $43 \leqq d \leqq 140$ is $\Delta r = 40.2 \pm 3.5$ arc msec. For the range $43 \leqq d \leqq 156$ it is $\Delta r = 44.1 \pm 4.2$ arc msec. The latter value is regarded as somewhat unreliable.

Combining the results from the diagonal oblateness component given in (*6*) with those from the vertical component gives the mean $\Delta r = 43.3 \pm 3.3$ arc msec and the oblateness $\Delta r / r = 4.51 \pm 0.34 \times 10^{-5}$ discussed above.

A great deal hangs on this result, no less than the validity of Einstein's general relativity! But the web of interpretation of this observation is so complex and the solar skin that we can see is so thin and so complex that no one will want to accept the above interpretation without supporting evidence. This is as it should be, but I take a measure of comfort from the large number of suggestions and criticisms that have been successfully disposed of. It seems quite unlikely that some new and revolutionary explanation will be found for the solar oblateness signal after such a long time during which so many have attempted without any particular success to find alternative explanations for it. But the key element is still missing—support from other accurate tests of relativity capable of distinguishing between Einstein's theory of gravitation and the scalar-tensor theory. Sufficiently accurate complementary tests should be available in a few years.

References and Notes

1. R. H. Dicke and H. M. Goldenberg, *Phys. Rev. Lett.* **18**, 313 (1967).
2. R. H. Dicke, P. G. Roll, R. Krotkov, *Ann. Phys.* (*N.Y.*) **26**, 442 (1964).
3. J. Ashbrook, *Sky Telesc.* **34**, 229 (1967); R. H. Dicke, *ibid.*, p. 371; E. J. Öpik, *Ir. Astron. J.* **8**, 29 (1967); R. H. Dicke, *ibid.*, p. 29; W. J. Cocke, *Phys. Rev. Lett.* **19**, 609 (1967); I. W. Roxburgh, *Nature (Lond.)* **213**, 1077 (1967); R. H. Dicke and H. M. Goldenberg, *ibid.* **214**, 1294 (1967); P. A. Sturrock and J. J. Gilvarry, *ibid.* **216**, 1280 (1967); R. H. Dicke, *Astrophys. J.* **159**, 1 (1970); B. R. Durney and I. W. Roxburgh, *Nature (Lond.)* **221**, 646 (1969); A. P. Ingersoll and E. A. Spiegel, *Astrophys. J.* **163**, 375 (1971); B. R. Durney and N. E. Werner, *Solar Phys.* **21**, 21 (1971); B. R. Durney, *Astrophys. J.* **183**, 665 (1973); R. H. Dicke, *ibid.* **180**, 293 (1973); G. A. Chapman and A. P. Ingersoll, *ibid.* **175**, 819 (1972); *ibid.* **183**, 1005 (1973); R. H. Dicke, *ibid.* **175**, 831 (1972); *ibid.*, in press; L. N. Howard, D. W. Moore, E. A. Spiegel, *Nature (Lond.)* **241**, 1297 (1967); P. Goldreich and G. Schubert, *Astrophys. J.* **150**, 571 (1968); K. Fricke, *Z. Astrophys.* **68**, 317 (1968); L. Mestel, private communication; T. Sakurai, *Publ. Astron. Soc. Jap.* **24**, 153 (1972); R. H. Dicke, *Astrophys. J.* **149**, L121 (1967); *Science* **157**, 960 (1967); *Astrophys. J.* **171**, 331 (1972); R. S. Kandel and S. L. Keil, in preparation.
4. R. H. Dicke, in *Stellar Rotation*, A. Slettebak, Ed. (Reidel, Dordrecht, Netherlands, 1970); *Annu. Rev. Astron. Astrophys.* **8**, 297 (1970).
5. ———, in *Proceedings of the International School of Physics "Enrico Fermi," Course 55*, B. Bertotti, Ed. (Academic Press, New York, in press.)
6. ——— and H. M. Goldenberg, *Astrophys. J. Suppl.*, in press.
7. U. J. Leverrier, *Ann. Obs. Paris* **5**, 1 (1859).
8. P. Jordan, *Astron. Nachr.* **276**, 1955 (1948); *Schwerkraft und Weltall* (Vieweg, Braunschweig, Germany, 1959); Y. R. Thirry, *C. R. Hebd. Seances Acad. Sci.* **226**, 216 (19[illegible] P. G. Bergmann, *Ann. Math.* **49**, 255 (1948); *Int. J. Theor. Phys.* **1**, 25 (1968); R. H. Dicke, *Phys. Rev.* **125**, 2163 (1962); R. V. Wagoner, *Phys. Rev. D* **1**, 3209 (1970); K. Nordvedt, Jr., *Astrophys. J.* **161**, 1059 (1970).
9. C. Brans and R. H. Dicke, *Phys. Rev.* **124**, 925 (1961).
10. R. H. Dicke and P. J. E. Peebles, *Space Sci. Rev.* **4**, 419 (1965).
11. S. Newcomb, *The Elements of the Four Inner Planets* (Government Printing Office, Washington, D.C., 1895).
12. R. H. Dicke, *Nature (Lond.)* **202**, 432 (1964).
13. G. M. Clemence, *Astron. Pap. Am. Ephemeris* **11**, 1 (1943).
14. R. H. Dicke, *Astrophys. J.* **159**, 1 (1970).
15. B. E. McDonald, *Astrophys. Space Sci.* **19**, 309 (1972).
16. E. J. Weber and L. Davis, Jr., *Astrophys. J.* **148**, 217 (1967); J. L. Modiesette, *J. Geophys. Res.* **72**, 1521 (1967).
17. R. H. Dicke, *Astrophys. J.* **171**, 331 (1972).
18. L. Mestel, in *Stellar Structure*, L. H. Aller and D. B. McLaughlin, Eds. (Univ. of Chicago Press, Chicago, 1965).
19. A. Clark, P. A. Clark, J. H. Thomas, N. H. Lee, *J. Fluid Mech.* **45**, 131 (1971).
20. R. Kraft, *Astrophys. J.* **150**, 551 (1967).
21. G. Wallerstein and P. S. Conti, *Annu. Rev. Astron. Astrophys.* **7**, 99 (1969); P. S. Conti, *Astrophys. J.* **152**, 657 (1968).
22. I. W. Roxburgh, *Icarus* **3**, 92 (1964).
23. H. H. Plaskett, *Observatory* **85**, 178 (1965); A. J. Deutsch, *Science* **156**, 236 (1967).
24. R. H. Dicke, *Sky Telesc.* **34**, 371 (1967); W. P Hirst, *ibid.*, p. 371.
25. R. H. Dicke, *Astrophys. J.* **176**, 479 (1972).
26. ———, *ibid.* **183**, 1005 (1973).
27. ———, *ibid.*, in press.
28. G. A. Chapman and A. P. Ingersoll, *ibid.* **183**, 1005 (1973).
29. R. H. Dicke, *ibid.* **180**, 293 (1973).
30. J. B. Rogerson, *ibid.* **134**, 331 (1961).
31. R. C. Altrock and R. C. Canfield, *ibid.* **171**, L71 (1972).
32. The "folded" function given in Fig. 8 is a moving mean, the day number d being incremented by ⅓.
33. The periodic autocorrelation function differs from the ordinary autocorrelation function by including in the correlation product all positive lags modulo p instead of the single lag p. That is, at the period p the periodic autocorrelation function is defined by $c(p) = \Sigma\ \delta y(d)\ \delta y(d + mp) / [\Sigma\ \delta y(d)^2 \cdot \Sigma\ \delta y(d + mp)^2]^{1/2}$, where $m = 1, 2, 3, \ldots$ and the sums are over all d and m for which data exist at both days; δy is the fluctuation with zero mean. Owing to the finite number of terms and to the multiple occurrence of the data from some days in the correlation sum, the distribution of $\ln[(1 + c)/(1 - c)]$ is not quite gaussian. The correction for multiple occurrence of data is difficult and only an upper bound is obtained.
34. Even more interesting is the fact that the correlation function derived from these two folded functions shows no hint of a zero-lag peak. This is a particularly sensitive test for the presence of the 25⅔-day periodically in F_c. Folding the data serves as a filter to reduce noise at frequencies other than those describing the periodicity (that is, 1/25.66, 2/25.66, . . . day^{-1}).

35. Supported in part by the Office of Naval Research and the National Science Foundation.